Article:
Khan, T, Tamura, Y, Yamamoto, H et al. (2 more authors) (2016) Friction and wear mechanisms in boundary lubricated oxy-nitrided treated samples. Wear, 368/9. pp. 101-115. ISSN 0043-1648

https://doi.org/10.1016/j.wear.2016.09.010

Friction and wear mechanisms in boundary lubricated oxy-nitrided treated samples

Thawhid Khan[1)*], Yukio Tamura[2)], Hiroshi Yamamoto[2)], Ardian Morina[1)] and Anne Neville[1)]

[1)] Institute of Functional Surfaces, School of Mechanical Engineering, University of Leeds, Leeds, LS2 9JT, United Kingdom
[2)] Materials Technical Centre, Development Division, Komatsu Ltd., Kanagawa 254-8567, Japan

*Corresponding author: mn09tak@leeds.ac.uk

Oxy-nitriding has been found to be an effective surface treatment technique, used widely in industrial applications due to its ability to prolong the performance lifetime of components. However there has been little work focussing on the potential synergistic effects on tribological behaviour between the treated layers after oxy-nitriding and anti-wear lubricant additives to optimise performance. The friction and wear behaviour of oxy-nitrided (QPQ), MoS_2 coated and plain steel samples were analysed. Scanning Electron Microscope (SEM), X-ray Photoelectron Spectroscopy (XPS) and Raman spectroscopy were employed to identify the morphologies and chemical compositions of the treated surfaces before and after testing. QPQ samples exhibited a lower friction coefficient and volume loss. The main mechanisms of these effects were attributed to the mechanical properties of the compound layer formed after the QPQ process and the possible influence of the greater concentration of FeS_2 within the tribofilm.

Keywords: Oxy-nitriding, MoS_2 coating, iron oxide, Zinc Dialkyldithiophosphate, FeS_2 layer

1. Introduction

With a range of coatings and heat treatments being applied to industrial parts running in the boundary (or mixed) lubrication regimes, it is important to understand the tribochemical interactions between the lubricant additives and treated surfaces. This allows the assessment of the effectiveness of selected surface treatments during operating conditions, alongside achieving efficient and effective performance from the component [1].

Hydraulic motors/pumps are key components within hydraulic systems, but they are hindered by their inefficiency which in some cases can be up to 15% [2]. High friction between interacting components can cause excessive wear and may also initiate seizure and complete failure of the motor/pump. Two key causes of seizure are identified as [3].

1. Entrapment of wear particles: High friction between interacting components can create excessive wear particles which may initiate seizure or cause the breakdown of the lubricating film [3].
2. When the speed of the system and/or the viscosity of the oil decreases, the lubricant film becomes very thin where it can reach a point where the entire load is supported by the interacting asperities of the contacting surfaces. This process can eventually initiate seizure [3].

Several mechanical systems are being modified to reduce friction amongst components whilst allowing them to operate at higher temperatures and running conditions. This is where surface improvement technology can play a crucial role in producing durable and optimum efficient systems [4, 5].

Zinc dialkyldithiophosphate (ZDDP) is one of the most effective anti-wear and extreme-pressure additive commonly applied to hydraulic fluids. The formation of a glassy phosphate film on running tracks due to interacting contacts helps determine the effectiveness of the wear reduction by preventing adhesion between surfaces and reducing stresses caused by surface asperities [1, 6]. The formation of the tribofilm through the interaction of ZDDP with a steel interface is influenced by the conditions such as applied contact pressure, additive concentration and temperature which would impact its thickness, physical and chemical properties [7]. Spikes [6] research showed that temperatures below 40°C ZDDP adsorbed physically and reversibly on to the surface however above 60°C a combined chemisorbed and chemically reactive film was formed, hence an experimental temperature of 80°C was used within this study. The interaction of ZDDP with solid surfaces could lead to the formation of different compounds such as iron sulphide or zinc/iron phosphate which could further impact the wear and friction behaviour of the tribofilm [1]. Iron sulphides are formed as part of extreme pressure reaction of the additive, present at critical spots of high stress [6].

There have been very few studies that investigate the interaction of iron oxide layers formed on a nitrided surface with ZDDP. This paper focusses on tribological and tribochemical interactions occurring between a modified steel surface and a fully-formulated hydraulic oil using tribometer tests, supported by chemical analysis to identify the mechanisms of low friction and wear behaviour. The two treatments chosen to treat the samples were either an oxy-nitriding (QPQ) heat process or a molybdenum disulphide (MoS_2) alongside a manganese phosphate (MnP) coating. Literature associates low friction with high wear, due to the application of soft running-in coatings/layers which are used as a friction control measure. In this study how to achieve and maintain low friction and wear using surface engineering techniques is discussed in the context of the oxy-nitriding and MoS_2 coating process. By understanding the tribochemistry at the interface, avenues to optimise the lubricant formulation for that particular surface treatment are opened up.

2. Experimental Methodologies

2.1 Materials and lubricants

The material used for this investigation is nitriding steel, generally used for components subjected to high friction and wear. The pin samples with semi spherical ends (sliding r = 10 mm x h = 20 mm) had a hardness of ~300HV_1 prior to treatment. A 10mm sliding radius for the pins was used to allow the application of contact pressures up to 2 GPa. To carry out the oxy-nitriding heat (QPQ) treatment on the samples, it involved using a cyanide/cyanate bath at 400-600°C to form a nitride layer (15 µm), followed by using a specialized nitrate – nitrite cooling salt bath to form an oxide layer (0.5µm) on top, which acts as a protective running-in coating (process highlighted in Figure 1) [8]. Another variant of the nitriding process was applied to the counter face plate samples. The 7mm x 7mm x 3mm plates were made from spheroidal graphite cast iron which were then gas nitrided (R_a = 0.6 µm). The treatment applied to the plates was not varied. The coupling of steel pins to cast iron plates represents friction pair components within a hydraulic motor.

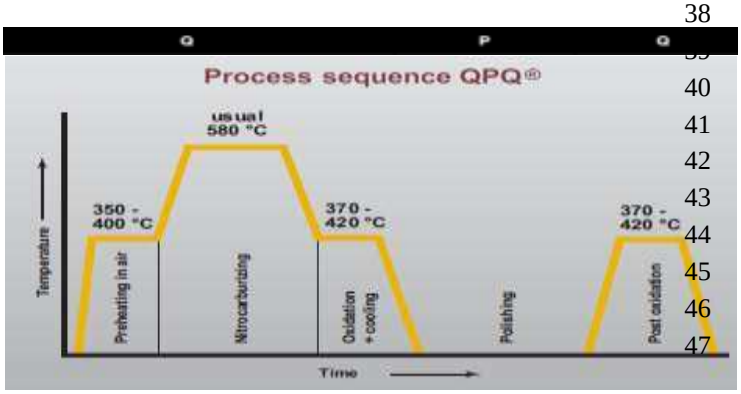

Figure 1. Salt bath nitriding (QPQ) heat treatment process [8].

The alternate treatment applied within this study involved using a gas-nitrided hardened pin sample, on which a manganese phosphate layer was formed on the surface using a phosphating process, followed by the spray-on application of a molybdenum disulphide (MoS_2) running-in paint coating (28μm) on top. This coating is typically used in systems where lubricants are deemed ineffective. The phosphate coating acts as a protective layer against corrosion and roughens the surface to encourage the firm rooting of the coating to the component surface. After the application of the coatings the samples are oven baked from 160-250°C. The key processes to the application of the coatings are highlighted in Figure 2 [9].

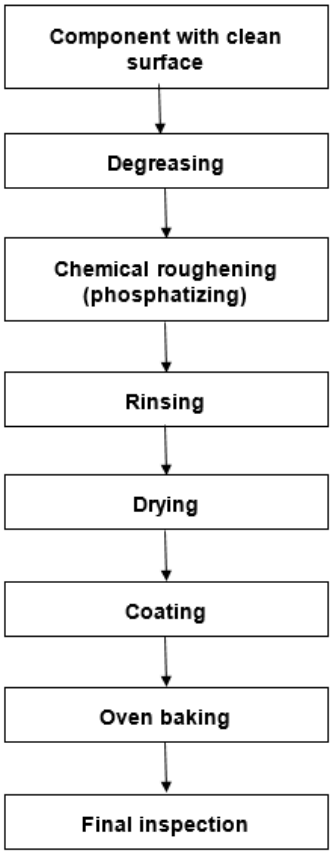

Figure 2. Schematic diagram for the application of the MoS_2 and MnP coatings [9].

The microstructure of the treated samples through their cross-sections have been examined using Scanning Electron Microscopy (SEM), which is also equipped with Energy Dispersion X-Ray Analysis (EDX) allowing the chemical analysis of the treated layers. The phases formed after the samples had been treated were characterized by a Siemens Bruker X-ray diffractometer (XRD) using Cu radiation. Microhardness measurements have been carried out with Micro Vickers microhardness tester using a load of 9.81 N (1 kg) across the samples cross-sections. The results are presented in Figure 3. The Taylor Hobson Form Talysurf was employed to measure the surface roughness of the samples.

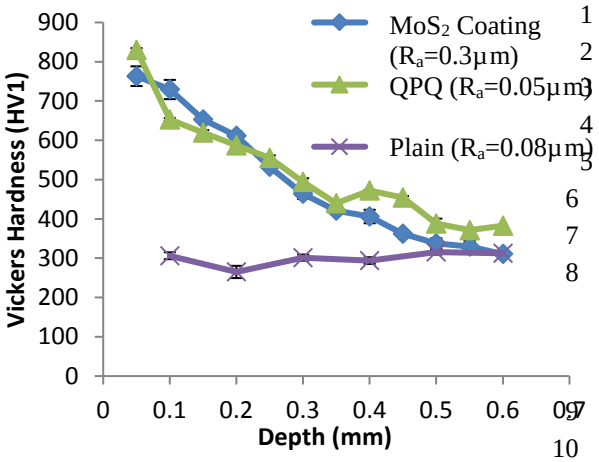

Figure 3. Comparison of the hardness through each of the treated samples cross-section and also their surface roughness.

This study used a fully-formulated hydraulic oil, with the additives being detergent, dispersant and the anti-wear additive ZDDP.

2.2 Tribometer Tests

Using a Cameron Plint TE77 (Figure 4) reciprocating tribometer with a pin-on-plate configuration to represent the sliding conditions of interacting components, the friction and wear behaviour of the treated samples could be investigated. In operation, the pins were the nitriding steel samples and the plates were composed from graphite cast iron, the treatments applied to both sets of samples are described above. The testing conditions are given in Table 1 and were derived from those used by Komatsu to mimic the operational conditions of a hydraulic motor. The addition of an extreme load (1.90 GPa) at 12 Hz primarily aimed at producing wear which penetrated past any coatings or treated layers present on the different samples, to allow differentiation of their impact on friction and wear behaviour.

Table 1. TE77 test conditions

Set up	Conditions
Stroke Length	7 mm
Sliding Speed	0.17 (12Hz) & 0.35 m/s (25Hz)
Hertzian Contact Pressure	0.92-1.90 GPa
Lubricant	Fully Formulated Oil
Dynamic Viscosity (100°C)	~0.030 Pa.s
Lubricant Temp.	80°C
Testing Time	2 h

The TE77 using a force transducer and program produces a data file of the friction force every 300 seconds for a duration of 2 hours. Each data file is composed of 1000 measurements taken every 0.3 seconds. The friction coefficient results were calculated when the system has reached steady state and were based on the last 30 minutes steady friction data. The lubricant was heated to 80°C using heating elements attached to the bath in which the samples were clamped down and flooded in lubricant.

The tests are carried out under the boundary lubrication regime which was defined by calculating the lambda ratio:

$$\lambda = \frac{h_{min}}{\sqrt{R_{q1}^2 + R_{q2}^2}} \quad (1)$$

where h_{min} is the minimum film thickness determined using the Dowson/Hamrock equation and R_{q1}^2 & R_{q2}^2 are the roughness of the interacting surfaces. For the lubrication regime to be within boundary condition; $\lambda<1$.

After testing the samples were washed in heptane to remove excess oil prior to surface analysis. All tests were repeated to achieve a good repeatability for the friction and wear behaviour.

2.3 Morphology and Topography Analysis

The changes in surface topography of the different samples were analysed using a Leica optical microscope and a Taylor Hobson Talysurf Profilometer, which allows the measurement of the depth of the wear scars formed on the pin samples.

2.4 Tribofilm Chemical Properties

Post experimental surface analysis included carrying out X-ray Photoelectron Spectroscopy (XPS) on the worn surfaces of the pin samples to identify the chemical species present in the tribofilms formed which could essentially affect friction and wear. A monochromatized Al Kα X-ray source was used to carryout high resolution scans for specific peaks. The beam line was focused in the centre of the wear scar in an area of 200 μm × 200 μm. The tribofilm was also etched and the charging effects in the results were corrected by fixing the C1s peak (adventitious carbon) at 284.8 eV. CasaXPS software which applies a Shirley algorithm to construct a background, through a curve fitting procedure, which is applied to the peaks identified. To accurately determine the chemical species present the peak's area and full-width at half-maximum (FWHM) were constrained.

2.5 Raman Spectroscopy

Raman spectroscopy was used to study the samples to confirm the formation of FeS_2, FeS and MoS_2 within the tribofilms formed on the different treated samples. Using a Renishaw Invia Raman spectrometer a 488 nm excitation wavelength laser source was used and different scans were taken in each spectrum using a spot size of 20 μm × 20 μm. To detect for the different chemical compounds a full scan from 100 cm^{-1} to 1650 cm^{-1}. WiRE software provided by the Raman equipment is used for curve fitting and peak position identification.

2.6 Focussed Ion Beam- Scanning Electron Microscope (FIB-SEM) Cross-Section Analysis

The FIB-SEM technique was used to observe the tribofilms formed on the surface of the different treated samples. A 1μm carbon film was deposited on to the center of the wear scar area of 20μm × 30μm at 320pA. Using a Ga^+ ion beam FIB milling was carried out to create an initial volume of 20μm × 20μm × 10μm at 30,000pA. Then a cleaning cross section was done at 1000pA. Further cleaning cross sections were carried out at 320pA with a volume of 25μm × 1.5μm × 8μm. The milled area was then imaged by SEM.

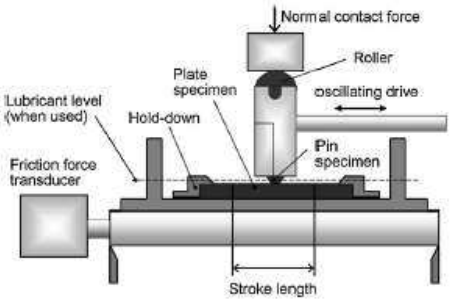

Figure 4. This figure shows the pin-on-plate configuration with the Cameron Plint TE77 and the main components of the tribometer [10].

3. Results

3.1 Surface characterization

Figures 5a & 6a show the SEM morphologies through the cross-section of each treated samples (QPQ and MoS_2). The plain (untreated) samples were shown to mainly be composed of pearlite and ferrite matrices. For the QPQ samples (Figure 5a) three distinctive layers are detected; on the very top surface a very thin black oxide layer of 0.5 µm thickness is present. This layer is not visible in Figure 5a, but had previously been identified by Komatsu and the treatment supplier. Underneath this layer is a 13 µm thick compound layer of a porous constitution. The final visible layer was a diffusion zone of approximately 250 µm thickness.

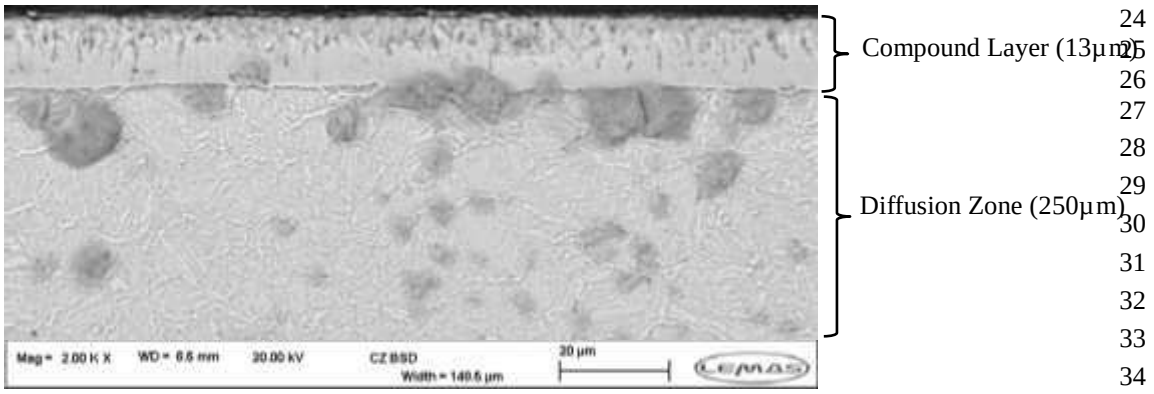

Figure 5a. SEM image profile through the cross-section of a QPQ sample.

X-ray diffraction (XRD) scans across the QPQ sample (Figure 5b) showed that the oxide layer was primarily composed of Fe_3O_4,whereas the compound layer was predominantly composed of ε-$Fe_{2-3}N$ with traces of γ'-Fe_4N. Using energy dispersive X-ray analysis (EDX) the C, Fe, N, O profiles through the QPQ samples can be mapped from the surface to the core (shown in Figure 5c). The distribution of C through the cross-section shows a high content at the surface then a quick decline. Using the nitrogen profile the compound layer thickness can be verified (13 µm – highlighted with dashed line) as the nitrogen peak begins to decline through the compound layer, and then levels off. The nitrogen profile is seen to have the lowest intensity compared to the others, which relates to the gradual diffusion of nitrogen from the surface to the core during the oxy-nitriding process. With the EDX scans carbon and nitrogen peaks are known to overlap, however due to the presence of the nitrided layer the nitrogen peaks can be clearly identified. At a 6 µm depth from the surface, an interesting phenomenon is observed where an increase of nitrogen

content is measured. This is due to iron atoms diffusing from the nitrided layer to surface which is being oxidised, this leads to a redistribution of nitrogen atoms in the compound layer and nitrogen atoms become abundant [11]. The gradual decrease of nitrogen through the specimen would hinder the formation of iron nitrides and fine nitrides which would account for the decrease in hardness through the specimen's depth.

From the iron profile it is possible to see that its intensity becomes stronger after a depth of 13 μm (circled in Fe profile – Figure 5c), where the compound layer ends and there is no real presence previous to this. This suggests that the compound layer has intermetallic/inert properties and the substrate has no real influence here. This changes at a greater depth where an increase in iron influence is observed.

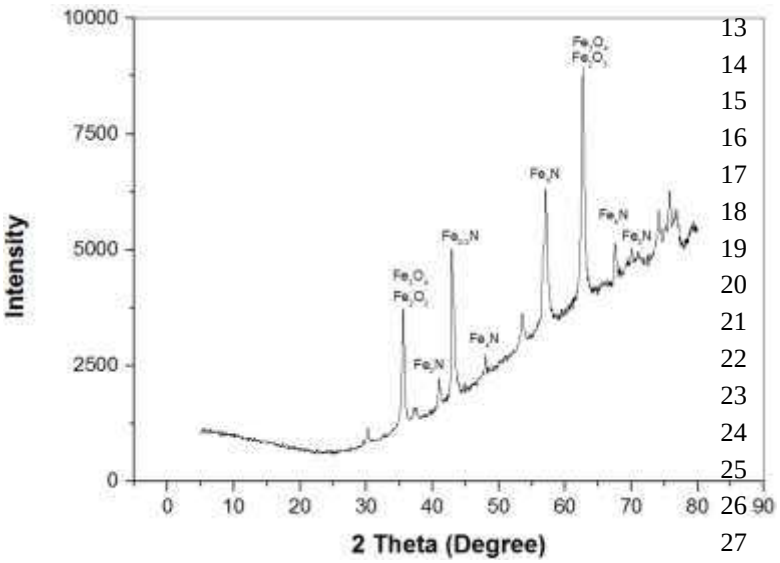

Figure 5b. X-ray diffraction pattern of a QPQ sample.

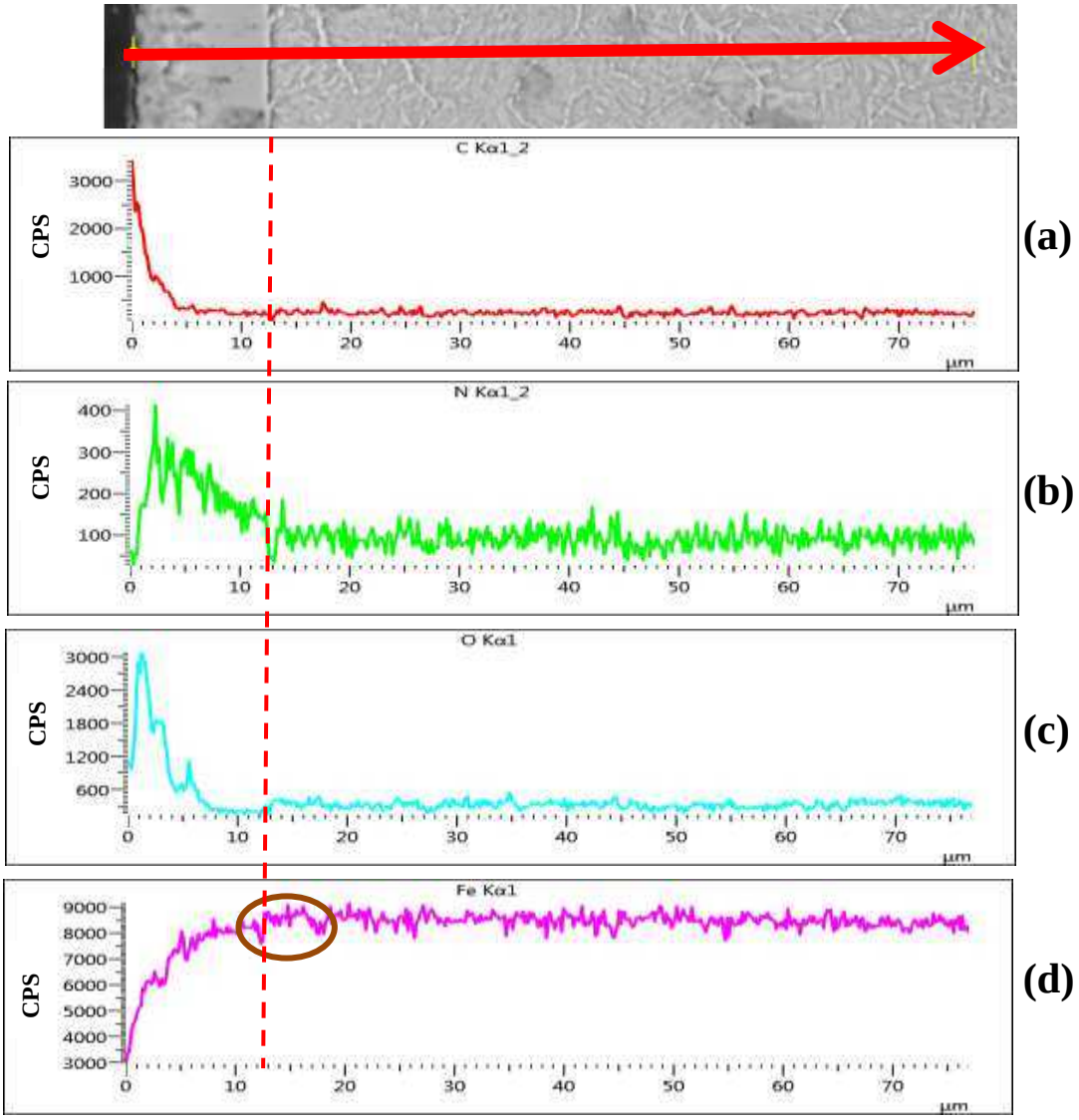

Figure 5c. The elemental profiles created using EDX through the cross-section of a QPQ sample: (**a**) C Profile (**b**) N Profile (**c**) O Profile (**d**) Fe Profile

Compared to the QPQ samples, the pins coated with MoS_2 (Figure 6a) possesses a thick granular layer (~28µm) followed by a thin ~4 µm MnP coating underneath. The total thickness of coatings applied is ~32 µm (highlighted with dashed line). Measurements taken using XRD (Figure 6b) identified the most dominant surface phase present as being molybdenum di-sulphide (MoS_2), MnP & $Fe_{2-4}N$.

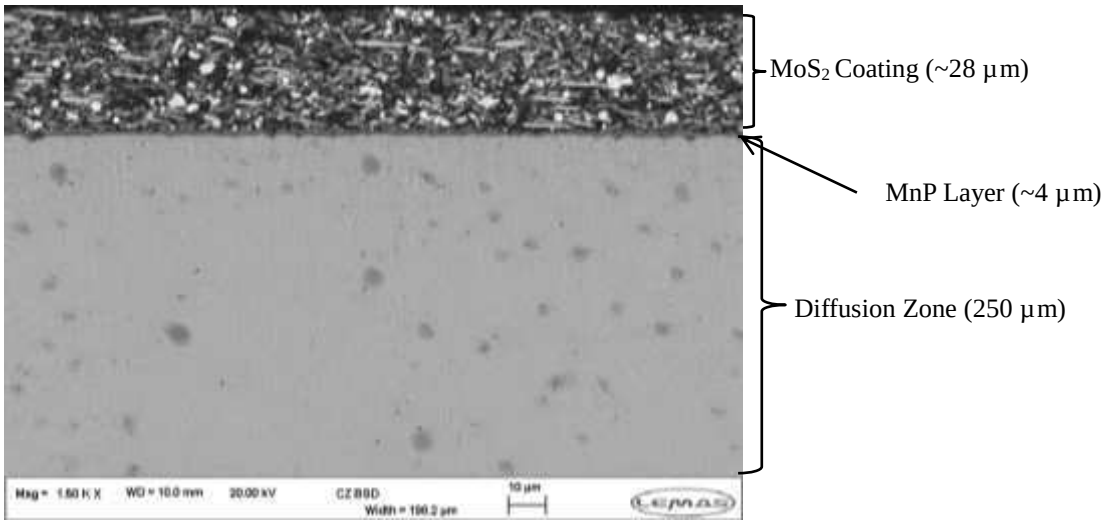

Figure 6a. SEM image profile through the cross-section of a MoS_2 coated sample.

17

Using EDX the Mo, S, C, Fe, N, Mn, P, O profiles through the MoS_2 samples can be mapped from the surface to the core (shown in Figure 6c). The line scan showed that the first ~10 µm of the MoS_2 coating was shown to be composed of C & O due to the sprayed on application of an MoS_2 paint coating and then as expected mainly consisted of Mo & S, as it is composed of molybdenum di-sulphide. However using a Mo & S profile map scan (Figure 6d) of the entire layer showed that MoS_2 was distributed through the entire coating from the top surface. The profiles show that the coating is ~28 µm thick, stopping where the Manganese Phosphate coating begins at a depth of ~28 µm. The Mo & S peaks overlap in EDX, but this indicates both elements are present, but it is not possible to quantify the intensity of each individual element. There is a high distribution of C through MoS_2 and there is a steep decline at the point where the Manganese Phosphate layer begins and remains at a very low level through the diffusion layer. An opposite trend is observed with Fe, where a very low presence is observed through the MoS_2 and manganese coating, but there is a quick increase at the boundary and through the substrate. At a depth of 28 µm from the surface after the MoS_2 coating there is a peak of manganese and phosphorous of about 4 µm thickness, which validates the thickness and position of the manganese phosphate coating.

The O and N profiles follow a similar trend through the MoS_2 coating, where there are significant peaks at the same points (3 µm & 18 µm depth), which indicates a significant presence of nitrogen and oxygen in the layer. There is an overall increase of nitrogen presence at the end of the MoS_2 and MnP coating, and through the substrate. This increase is due to the original application of a gas nitriding treatment to the substrate, before the nitride layers were removed. Another significant peak appearing in the O profile when the manganese phosphate coating begins, this indicates the presence of oxygen in the layer supporting the results shown from using XRD.

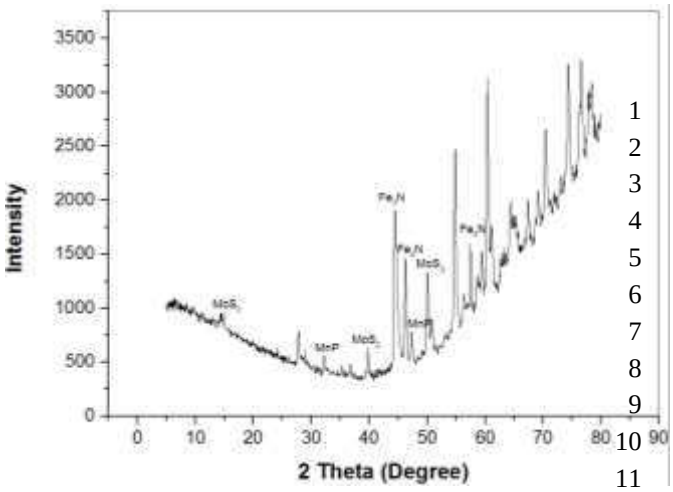

Figure 6b. X-ray diffraction pattern of a MoS_2 sample.

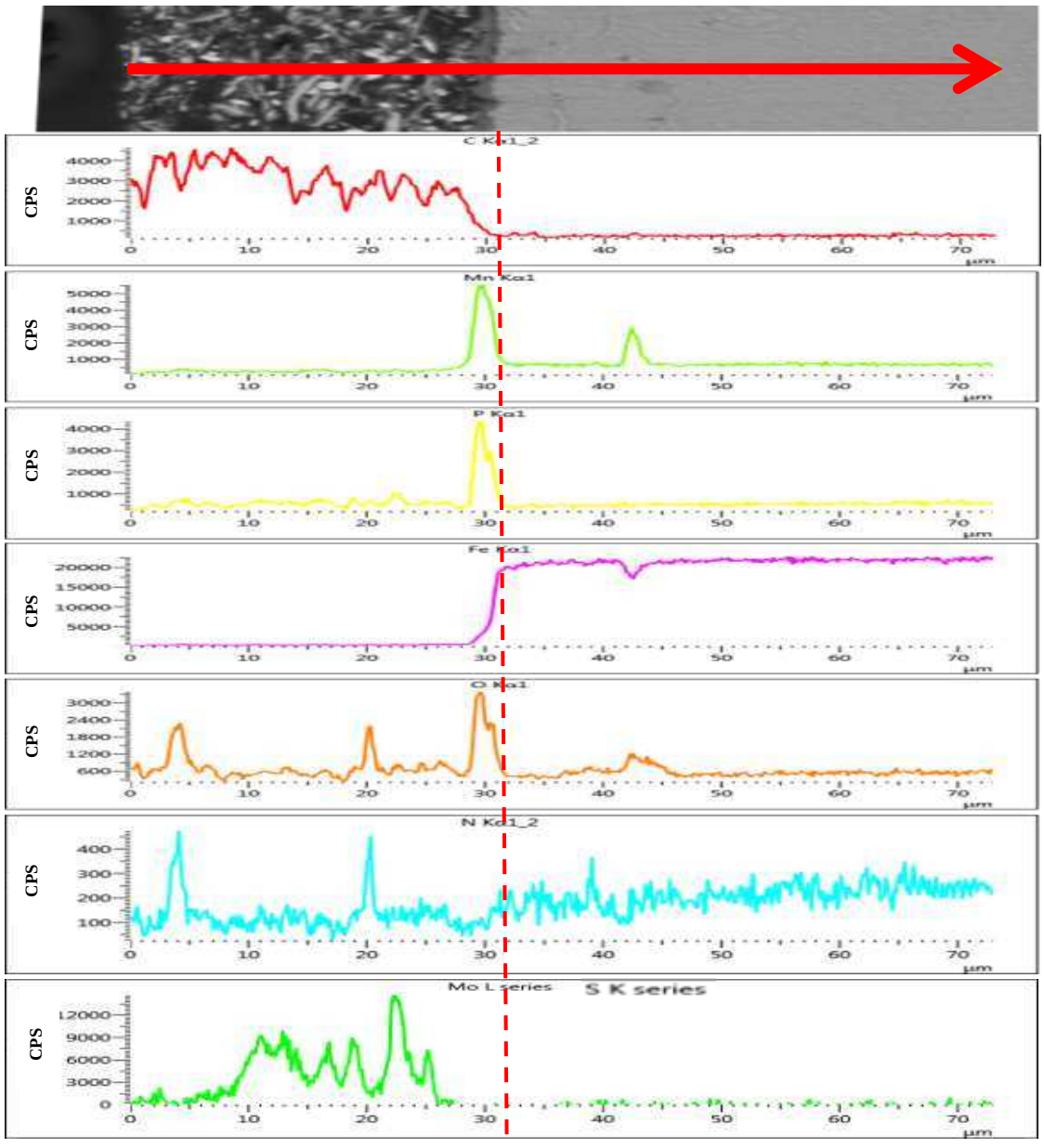

Figure 6c. The elemental profiles created using EDX through the cross-section of a MoS_2 coated sample: (**a**) C Profile (**b**) Mn Profile (**c**) P Profile (**d**) Fe Profile (**e**) O Profile (**f**) N Profile (**g**) Mo & S Profiles

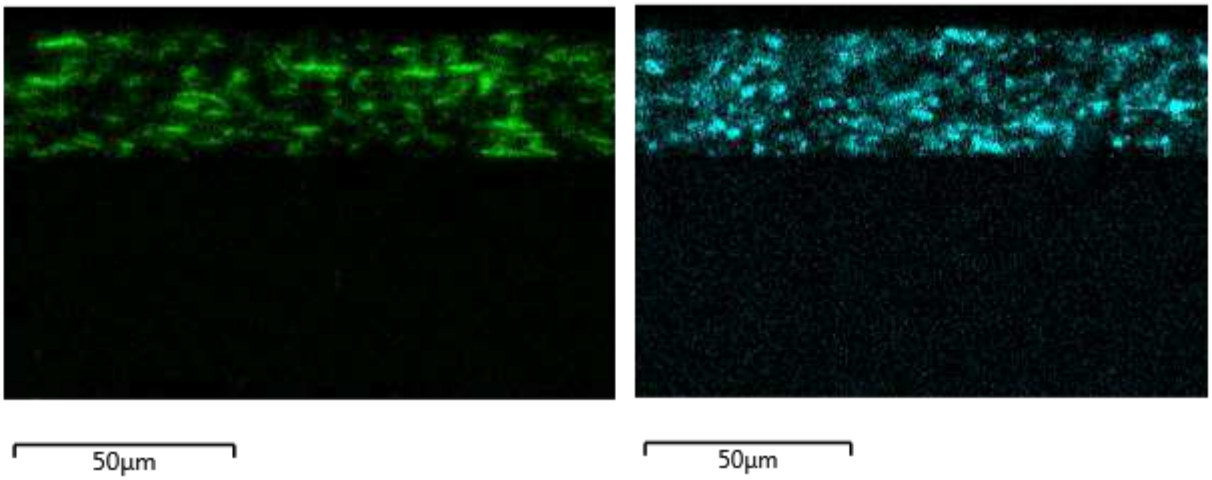

Figure 6d. EDX map of Mo & S profiles through the cross-section of the MoS_2 coated sample.

3.2 Friction evaluation

Figure 7a highlights the typical change in behaviour over time observed with the three samples during the complete duration of the test. Generally with the plain samples friction remains steady throughout with a slight increase later in the test. With the QPQ and MoS_2 coated samples generally there is a running in period after which friction drops and remains steady for the rest of the test.

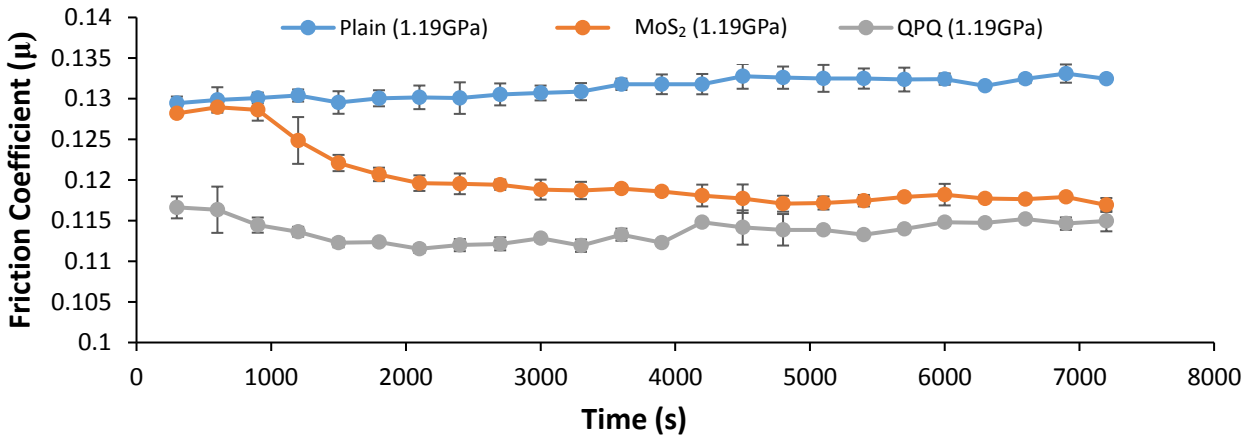

Figure 7a. Friction coefficient vs time results over 2 hrs with the three samples at a 1.19 GPa contact pressure and sliding frequency - 12 Hz.

The average friction coefficients for the untreated and treated samples in the stable stage (last 30 min of the test) under various contact pressures and sliding speeds are shown and compared in Figure 7b. It is observed that the general trend is that QPQ samples produce the lowest friction results compared to the MoS_2 -coated and plain samples, which confirms the role of the oxy-nitrided heat treatment in friction reduction. This general trend is observed at the different contact pressures and sliding speeds. With MoS_2-coated samples as the contact pressure is increased a drop in friction is consistently observed. For the untreated and MoS_2 -coated samples the friction coefficient values are comparable across the different testing conditions.

A change in trend is observed at the extreme contact pressure of 1.90 GPa which was applied to simulate an environment where the compound layer of the QPQ sample is removed. At this testing condition the MoS_2 sample has a lower friction coefficient than the plain and QPQ samples. The friction value of the QPQ value was also the highest observed when compared to the other contact pressures applied. This increase in friction is highlighted in Figure 5c.

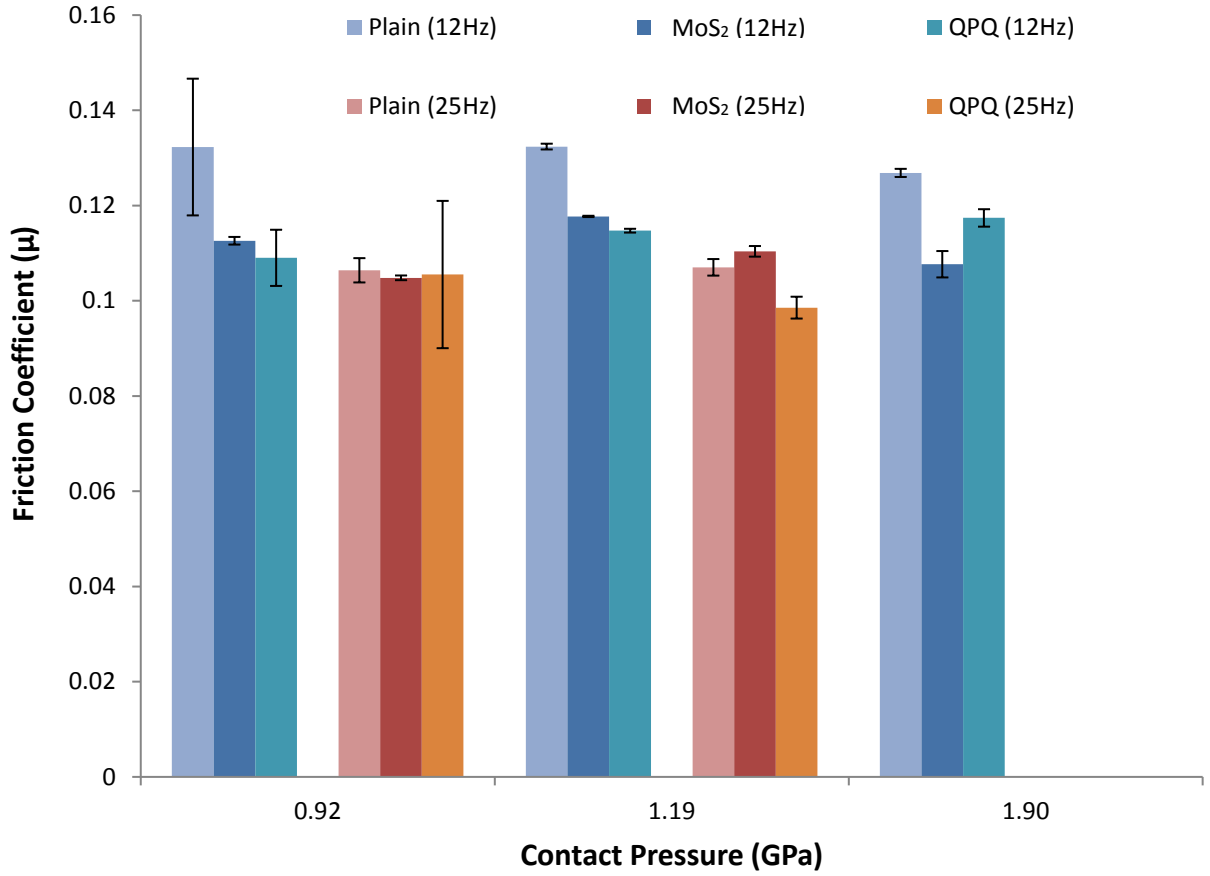

Figure 7b. Friction coefficient results from experiments when the applied load and sliding frequency are varied using fully formulated lubricant with three types of samples at 80°C.

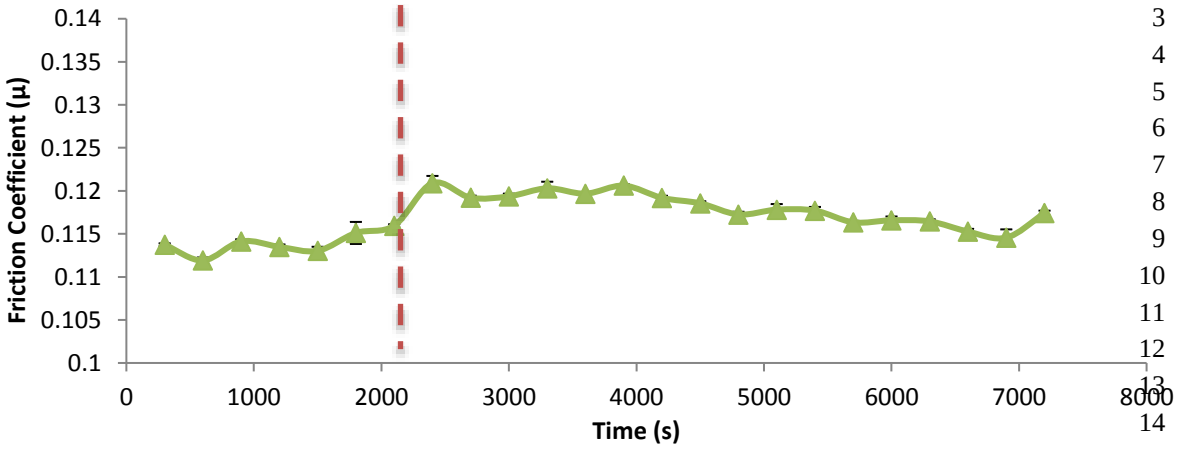

Figure 7c. Friction coefficient result for the QPQ sample when an extreme pressure (1.90 GPa) was applied at a sliding frequency of 12Hz. The line highlights the increase in friction after a period of 2000 seconds.

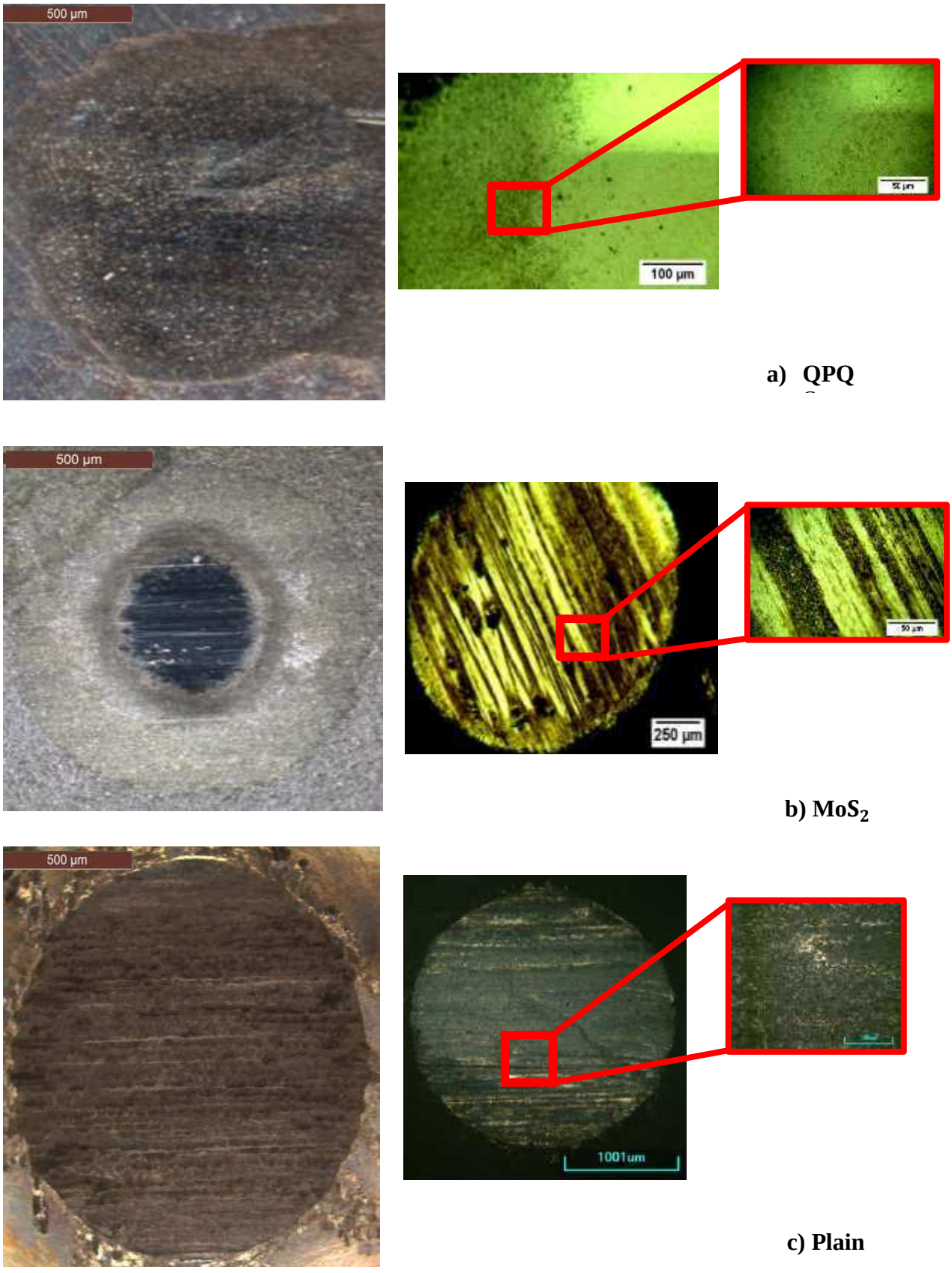

Figure 8. Optical images of the wear scar regions of the different treated pin samples when a 1.19 GPa contact pressure was applied at 12 Hz.

3.3 Wear results

Using an optical microscope the worn surfaces of the different samples (Figure 8) were analysed. With the QPQ pin (Figure 8a) a smooth surface is observed compared to the alternative samples, alongside a patchy thin tribofilm formed on top. With the MoS_2 coated samples (Figure 8b) it is possible to see a deeper penetrating wear scar, with higher magnification images showing the exposure of the substrate surface alongside the patchy remnants of the coating. The images show the delamination of the coating & scoring of the exposed surface. The plain samples (Figure 8c) show the exposure of a rough surface with the presence of a thick tribofilm.

The depth profile measurements using Talysurf (Figure 9) showed that the QPQ pins had the lowest wear depths, compared to the other samples where the loss was significantly higher, with the plain samples showing the greatest loss. Generally, the wear depths of the pins increased with the application of higher loads and frequencies. With the QPQ pins the wear depth was mainly contained within the compound layer, rarely reaching the diffusion zone. This is in contrast to the MoS_2 coated samples where the coating did not survive testing and in almost every case the wear depth penetrated into the substrate material. However with the application of the extreme contact pressure 1.90 GPa, Figure 9 highlights that the wear depth for the QPQ penetrates into the diffusion zone.

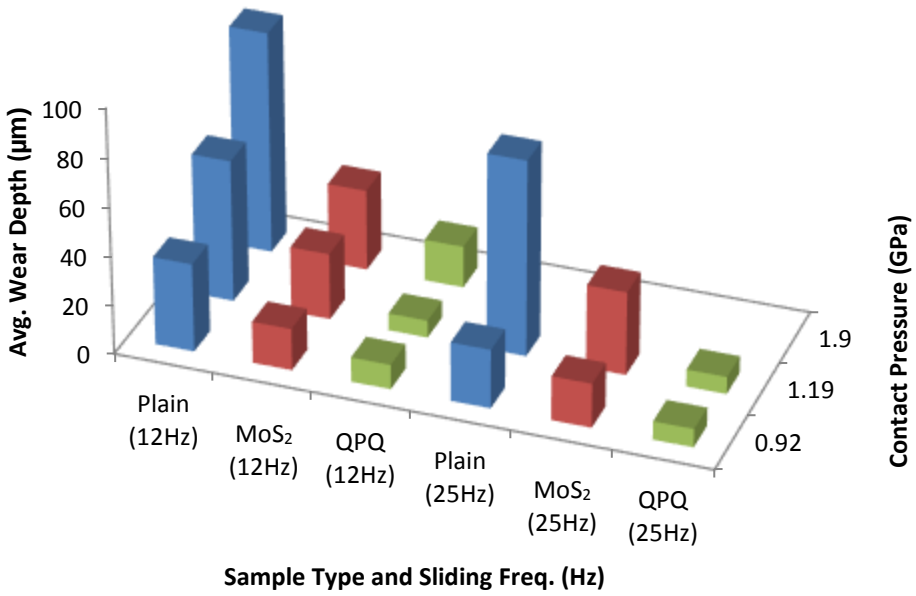

Figure 9. Wear depths (max error: $\pm$**5.7** µm) of the three types of pins when contact pressures 0.92-1.90GPa are applied at a 12Hz & 25Hz sliding frequencies using fully formulated lubricant at 80°C.

3.4 Tribofilm analysis

The cross section of the tribofilms formed on the different pin sample types were analysed by FIB-SEM. Figure 10 shows the images where cross sections of the anti-wear (AW) tribofilms formed were made by FIB milling and then examined using SEM. With the QPQ samples no significant tribofilm was visible in the areas analysed, supported by EDX scanning showing no presence of phosphorous and zinc which are the common elements associated with the formation of a glassy phosphate tribofilm, however there is the presence of sulphur peaks which is commonly associated with ZDDP. When using XPS to analyse the worn surface, the presence of a phosphate tribofilm was detected. With the MoS_2-coated sample a ~62 nm thick film was identified and EDX showed a strong presence of phosphorous and zinc. With the plain samples the tribofilm was identified and analysed at two points, having thicknesses of ~104 nm and ~194 nm respectively and EDX verified the presence of a phosphate tribofilm. XPS carried out on the worn surfaces of these two samples confirmed the presence of a ZDDP formed tribofilm.

In the images where the tribofilms were identified two dominant layers were observed. In each image the top layer is the tribofilm followed by the steel substrate underneath. A thicker non-uniform film was found to be formed on the plain sample which had the lowest surface hardness. Under boundary lubrication conditions, ZDDP reacts with the rubbing steel surface forming a tribofilm. This tribofilm is generally composed of mainly a mixed iron and zinc polyphosphate glass forming a pad-like structure. Long chain length organic and inorganic polyphosphates compose the outermost layer whereas the rest of the pad is composed of short chain length polyphosphates known as ortho- and pyrophosphates. The surface is protected by the sacrificial properties of the tribofilm [7].

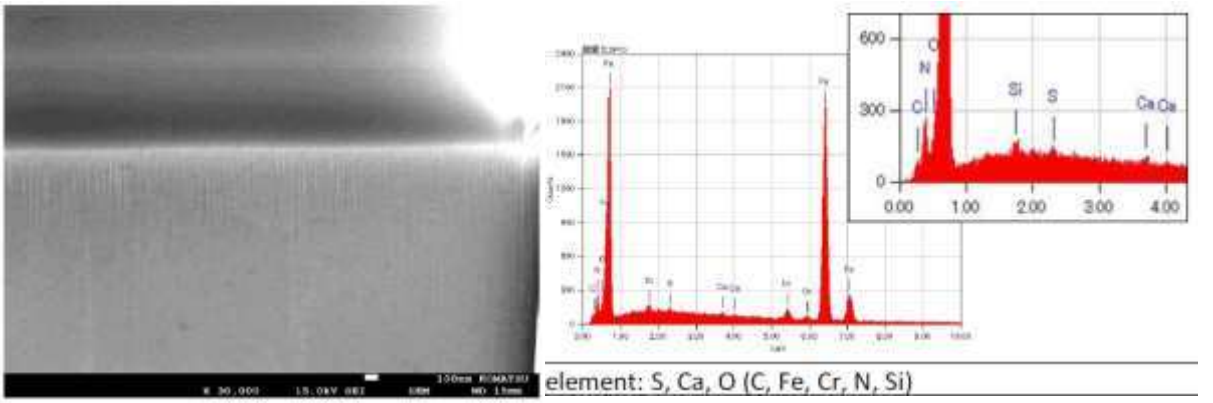

(a) QPQ

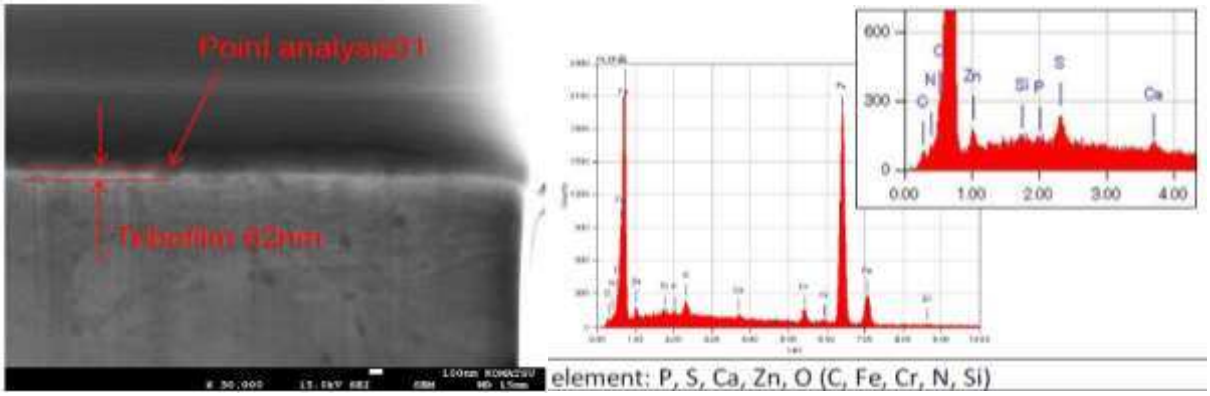

(b) MoS_2

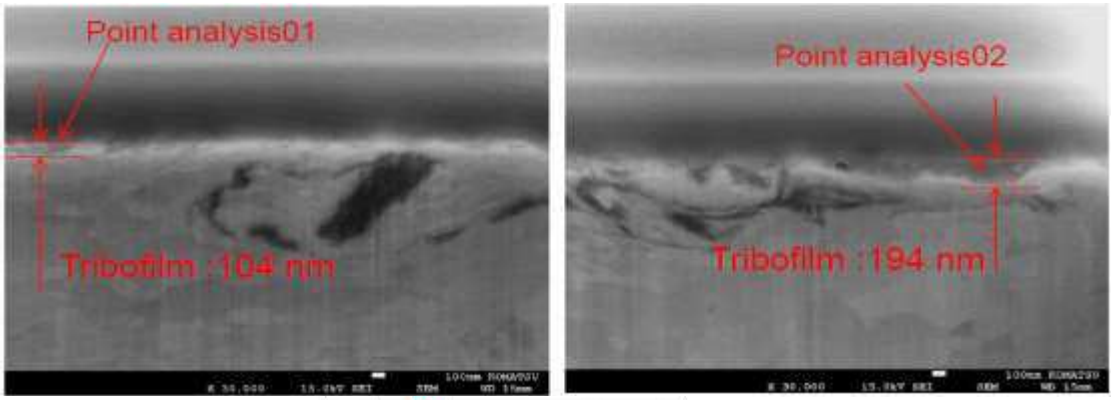

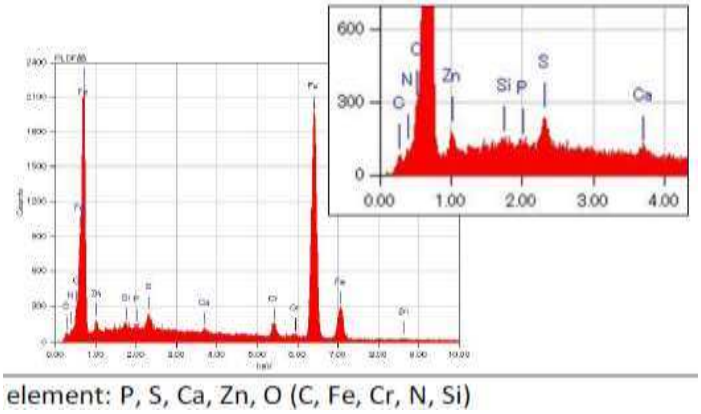

(c) Plain

Figure 10. FIB-SEM & EDX images of the tribofilms formed on the surface of the different treated samples at 1.19GPa contact pressure and 12Hz sliding speed.
(**a**) QPQ Samples (**b**) MoS_2 Coated Sample (**c**) Plain Sample

XPS was used to analyse the changes in chemical states of elements on the different treated samples worn surfaces. The results presented here focus on when an applied pressure of 1.19 GPa and a sliding speed of 12 Hz are applied as the tribochemical findings were representative of the findings of all contact pressures used at the lower sliding frequency. Etching times of 0 min, 0.2 min, 0.4 min and 0.8 min, were used to penetrate the depth of the tribofilm. Interestingly the presence of a phosphate anti-wear tribofilm was identified using XPS on the QPQ samples (Figure 12). This is most likely due to the larger area analysed and due to XPS being a more surface sensitive technique than EDX it was able to detect a relatively thin tribofilm. The tribofilms formed for all types of samples show the presence of ZnS/ZnO/Zn-phosphates and also the presence of sulphide and sulphate formation which are expected to appear and in agreement with EDX results (Figure 10). The tribofilm can mostly be classed as being composed from inorganic amorphous pyrophosphates associated with Zn and S [12].

With QPQ samples Fe 2p peaks were easily identified from the very top surface and through the tribofilm, whereas for MoS_2 coated samples Fe peaks were not detected until the samples had been etched for either 0.2 min or 0.4 min. The inability to detect Fe at the top surface of the MoS_2 samples indicates the formation of a thicker tribofilm than with QPQ samples as supported by the FIB-SEM findings. Overall the presence of Fe was significantly higher in the tribofilms of the QPQ samples, but the common chemical states found in the tribofilms of both types of samples were Fe_2O_3, FeO & FeS_2 (Table 2). With the presence of sulphides in the tribofilm and using Raman as a secondary technique it was possible to confirm the formation of FeS_2 species instead of metallic species. The plain samples had a higher Fe at% than MoS_2 coated samples (Figure 11). The Fe chemical states found within the plain sample tribofilms were the same as the previous samples with the additional presence of FeS. The detection of FeS_2 within the plain samples tribofilm is more common than with MoS_2-coated samples, but the at% is significantly lower than with QPQ samples at all etching periods which could be due to the formation of a thin film on the latter samples.

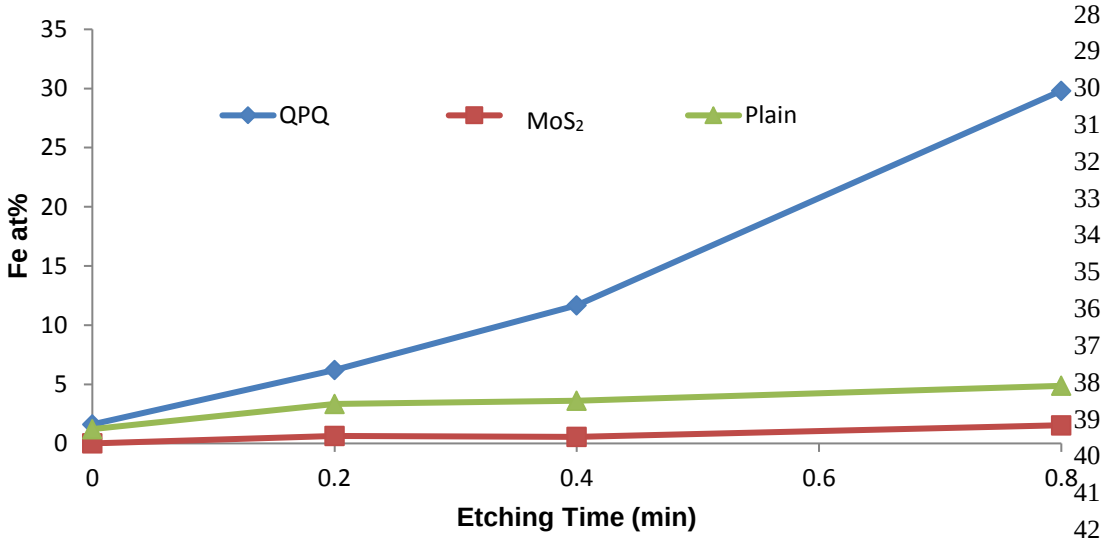

Figure 11. Compares the Fe at% for the three treated samples at four etching times, at 1.19 GPa contact pressure and 12Hz sliding frequency using XPS.

For the QPQ and Plain samples the key elements identified were carbon, oxygen, phosphorous, sulphur, zinc, iron, calcium and nitrogen. These elements were also present in the tribofilm formed on the samples which had been coated with MoS_2 with the exception of nitrogen. With the QPQ

samples the N 1s peaks only showed the formation of organic species on the unworn surface and within the thermal film formed. However after testing the tribofilm consisted of nitrides and organic species. With the Plain samples the presence of organic species were detected only at the very top of the tribofilm but not through its depth. Using XPS no chemical species of Molybdenum are detected in the tribofilm of the MoS_2 coated samples before and after testing. The main chemical species identified in both samples tribofilms are listed in Table 2:

Table 2. General binding energy values for compounds relevant to the tribofilms formed on the worn surfaces of all treated samples [1, 13].

Elements	BE / eV ($\pm$0.3eV)	Compound	QPQ	MoS_2 Coated	Plain
Fe 2p	706.8	FeS_2	✓	✓	✓
	709.4	FeO	×	✓	✓
	710.7	Fe_2O_3	✓	×	✓
	712.1	FeS	×	×	✓
Ca 2p	347.0	$CaCO_3$	✓	✓	✓
O 1s	529.6	Oxide	✓	✓	✓
	531.3	NBO	✓	✓	✓
	532.4	BO	✓	✓	✓
S 2p	161.7	Sulphide	✓	✓	✓
	168.3	Sulphate	✓	✓	✓
P 2p	133.4	Phosphate	✓	✓	✓
Zn 2p	1021.7	ZnS/ZnO	✓	✓	✓
N 1s	397.8	Nitride	✓	×	×
	399.7	Organic Species	✓	×	✓

The presence of an MoS_2 coating and FeS_2 compounds may influence the improved wear and friction behaviour seen with the MoS_2 coated and QPQ samples.

To understand the formation of the ZDDP tribofilm, the phosphate glass can be characterized. The glass polymerization number (n) can be calculated using the (bridging oxygen) BO (P-O-P)-to-(non-bridging oxygen) NBO (-P=O and P-O-Zn) ratio, Equation (2):

$$BO/NBO = (n-1)/2(n+1) \quad (2)$$

For n=1, the glass is an orthophosphate; for n=2 or higher the glass is a pyrophosphate or a metaphosphate [1]. With all types of worn samples in general pyrophosphate chains were formed, but QPQ treated samples produced shorter chain length of polyphosphate tribofilms (BO/NBO ratios - Figure 12). Crobu et al [7] showed that with higher oxide content the average chain length of the phosphates decreased. Within this study QPQ samples showed higher presence of oxides further supporting the indication of the presence of short phosphate chains (O 1s peaks – Figure 12). The thermal tribofilm formed on the unworn nitrided surface was of a longer chain length than when the surface had been worn, whereas with the MoS_2 coated and plain samples the unworn thermal samples produced shorter chained polyphosphates. It has been acknowledged that non-bridging oxygen can have P-O-S bonds which would affect the BO/NBO ratio, however within this study the influence was assumed to be negligible as it was not detected.

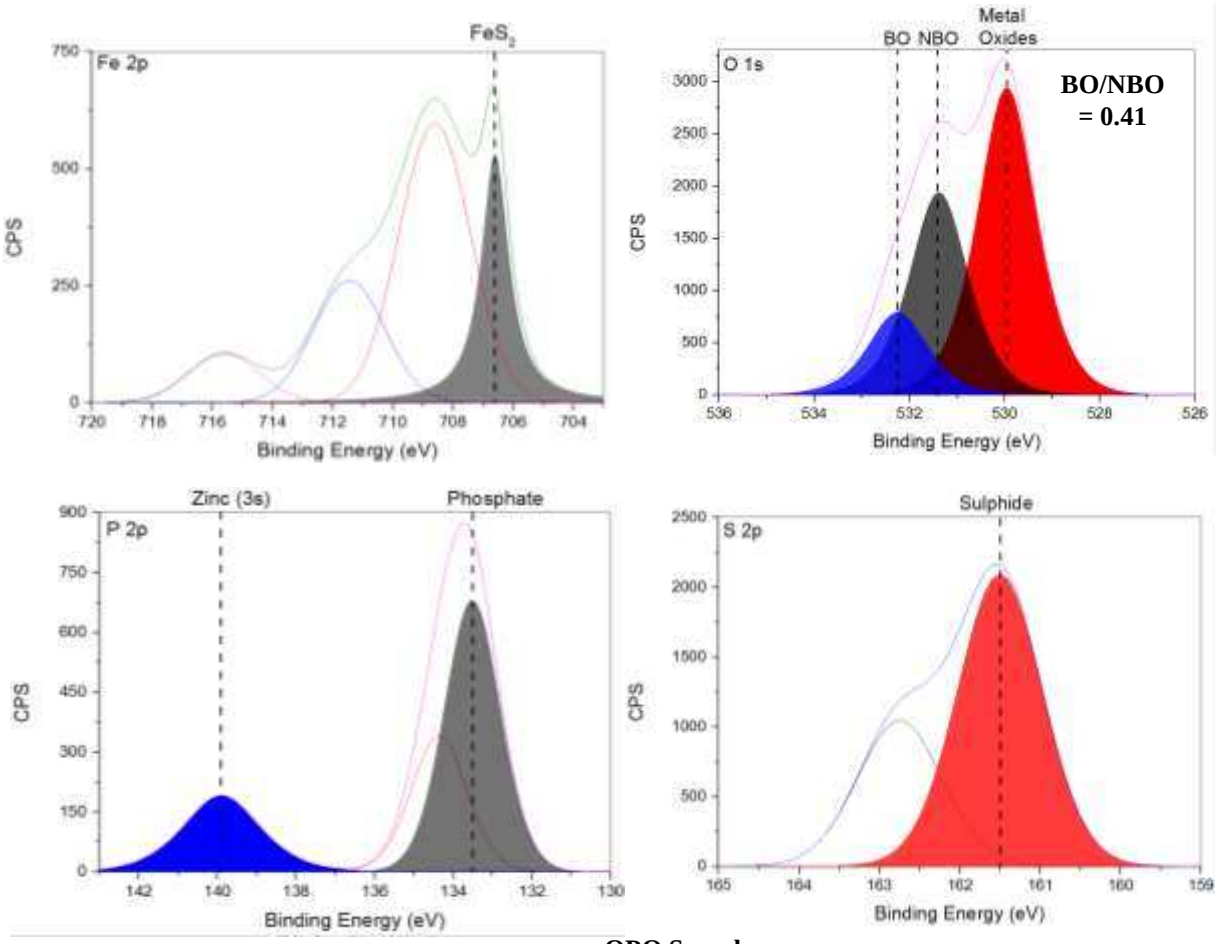

QPQ Sample

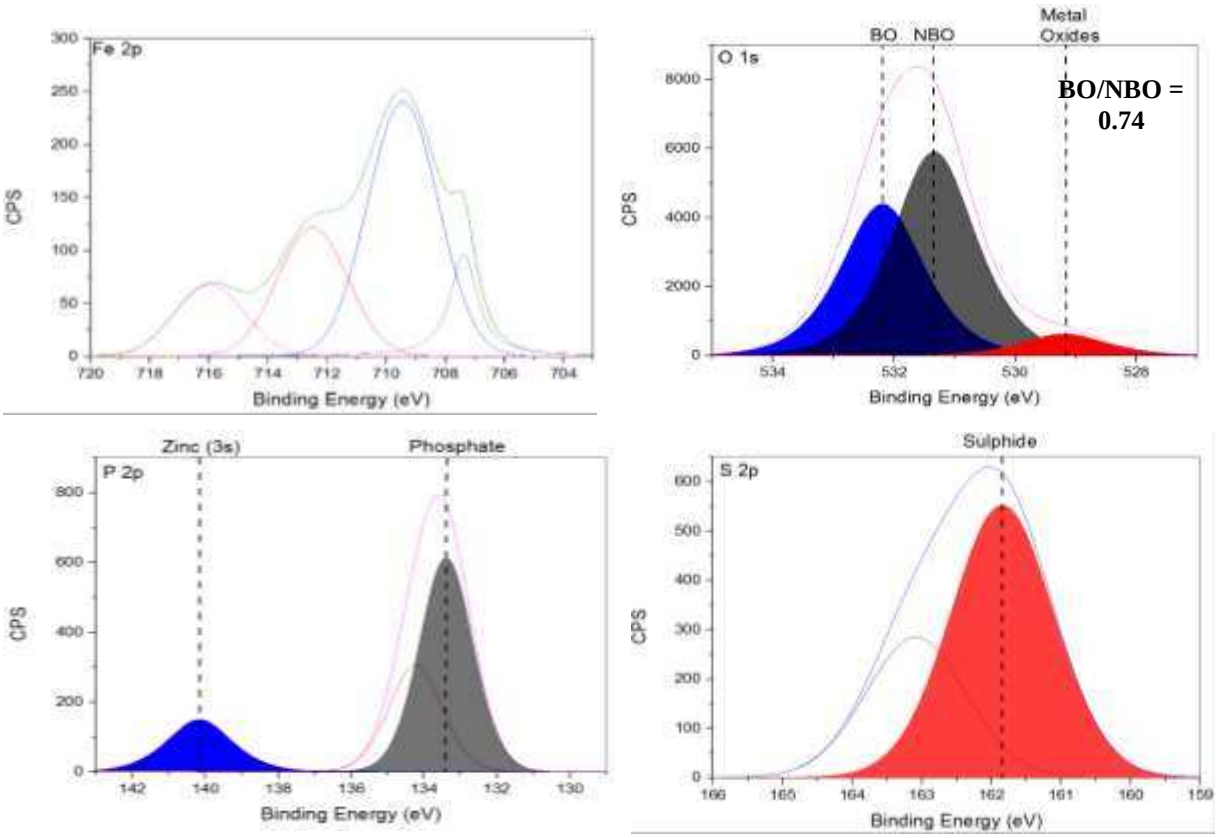

MoS_2 Coated Sample

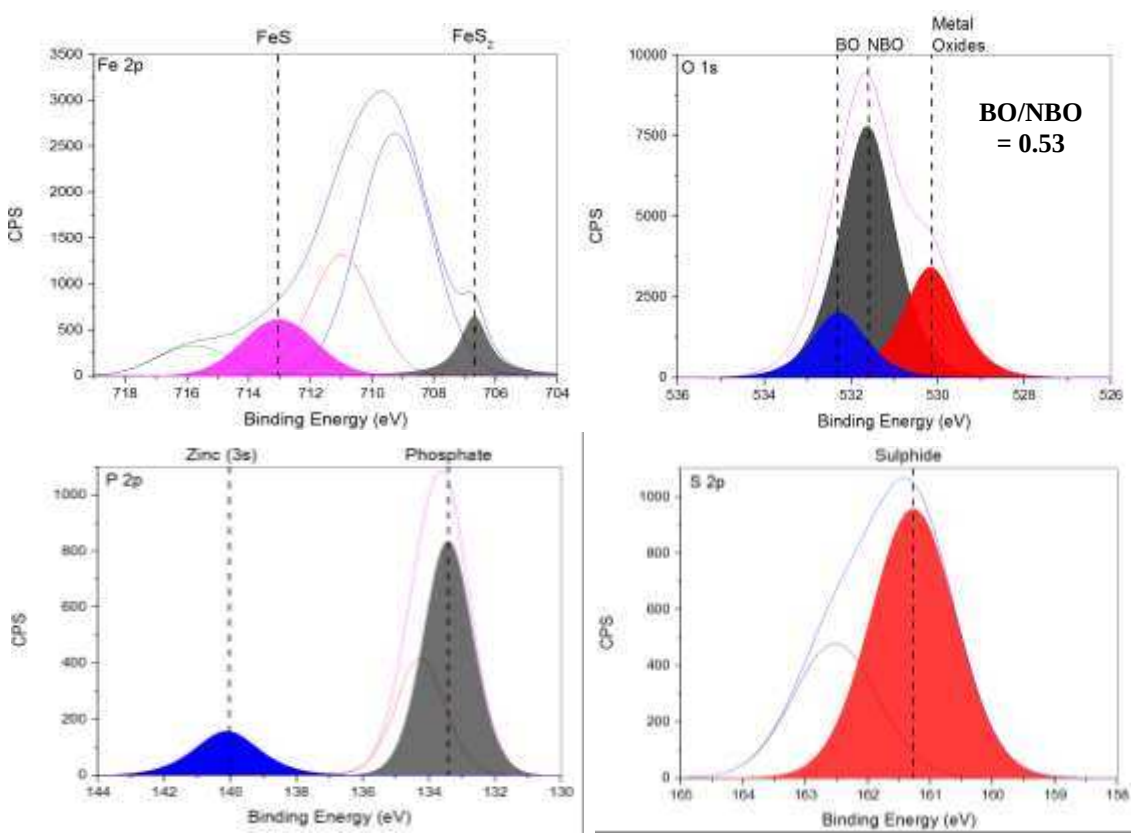

Figure 12. XPS Fe 2p, O 1s, S 2p and P 2p spectra of the tribofilms formed on the different treated samples at an applied contact pressure 1.19 GPa and 0.2 min etching time.

Raman spectroscopy was carried out to confirm the presence of key chemical compounds such as FeS_2, FeS & MoS_2 within the tribofilms formed by taking surveys of a wide coverage of the wear scars of the pins (Figure 13). With the QPQ samples the Raman peaks of FeS_2 were centered at 340 cm^{-1} and 373 $cm^{-1}$and were clearly identified [14], compared to the MoS_2 coated samples where a broad peak was detected, supporting the XPS and EDX findings that FeS_2 was present but at a smaller quantity than in the QPQ tribofilms. However the Raman peaks of MoS_2 were clearly identified at 384 cm^{-1} and 409 cm^{-1} [14], XPS had been unable to detect its presence this may have been due to the position of X-ray spot on the tribofilm or due to the formation of a thick tribofilm. With the plain samples no clear FeS_2 signal was identified, whereas two FeS peaks centered at 207 cm^{-1} and 283 cm^{-1} supporting the XPS findings that FeS compounds were present [15].

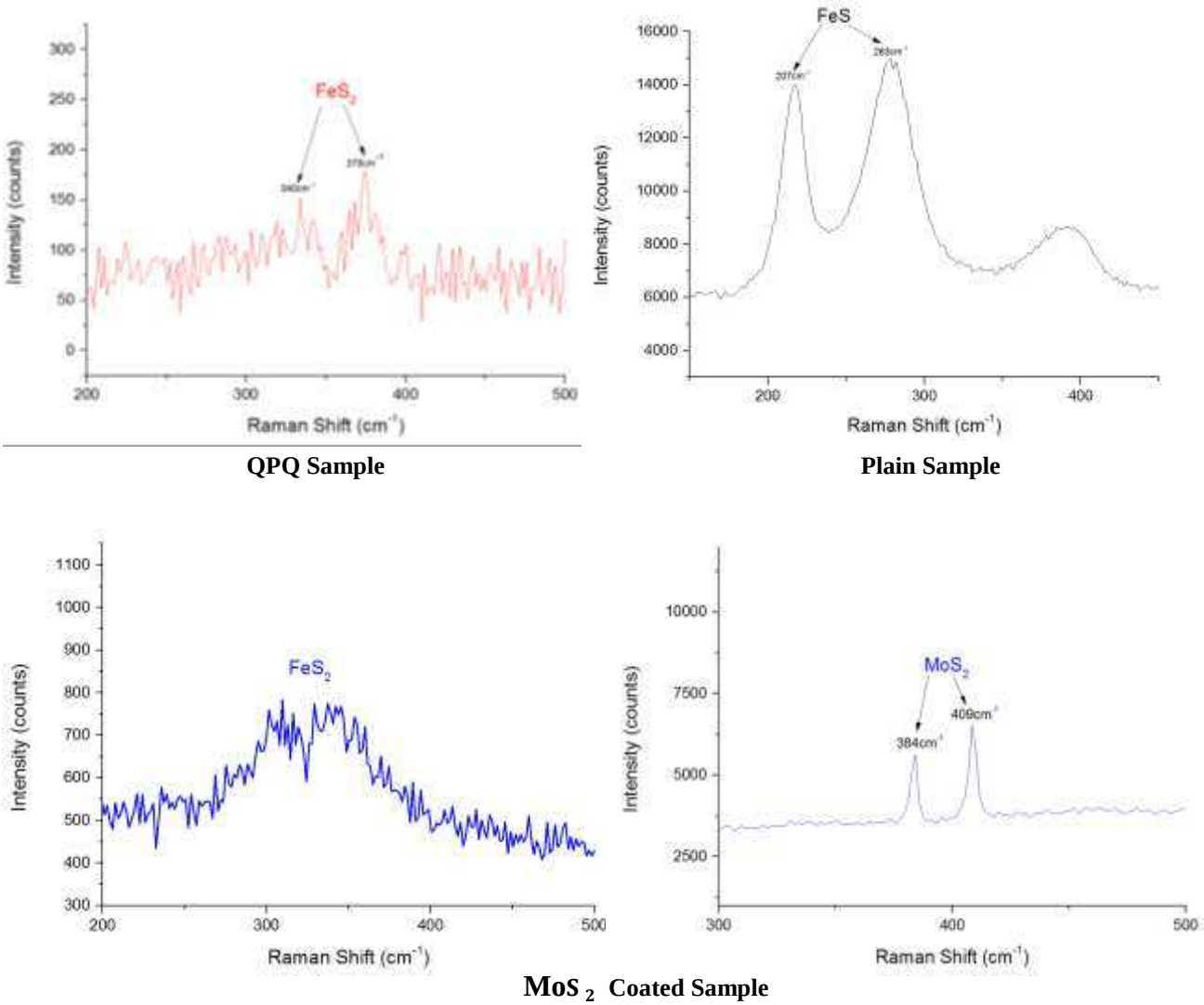

Figure 13. Raman spectra of different treated samples for FeS_2, FeS & MoS_2 compounds within the formed tribofilms of the pins tested at a contact pressure 1.19 GPa and 12 Hz sliding frequency.

4. Discussion

The tribological behaviour observed with the different treated samples is due to a combination of factors such as the surface mechanical properties alongside tribochemical interactions with the lubricant used. The following sections discuss this study's findings of the role the factors play in the friction and wear behaviour observed.

4.1 Friction and wear mechanisms

The lower friction observed with the presence of a MoS_2 layer is owing to its application on to a hardened substrate and the formation of a transfer film on the frictional counter-face. Using a material of high hardness would ensure contact loads are essentially supported by the contact material instead of the formed film. In this study the MoS_2 and MnP coated pins were hardened using gas nitriding before the nitrided layers were removed. The easy shear between lamellae within the formed transfer film (MoS_2) is deemed responsible for low friction behaviour [16, 17].

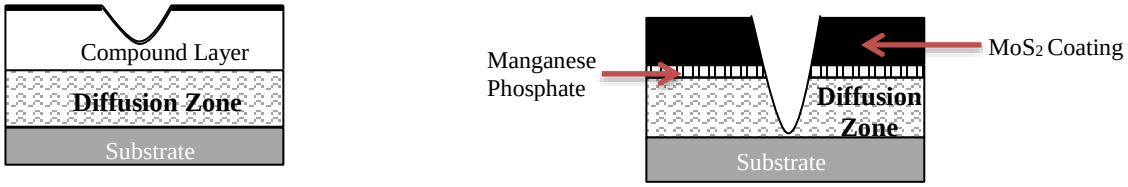

a) QPQ Sample b) MoS_2 Coated Sample

Figure 14. Cross-sectional scheme of *treated pin sample's worn surface.*

The properties of the layers formed after treatment (Figure 14) seem to play an influential and significant factor with wear and friction results observed. The influence of mechanical properties of the compound layer, when present with QPQ samples after testing, can be deemed to play a significant role in producing lower friction and wear results than the MoS_2 coated samples. Qiang et al [18] reported that the formation of a ε-phase containing compound layer with non-metallic properties makes it difficult for metallic counterparts to adhere with. This combined with a lamellar close packed hexagonal microstructure, which is easy to slide and to run in along the base plane would help to reduce the heat produced by friction. These characteristics would help to contribute to the low friction behaviour observed. By applying an extreme contact of 1.90 GPa so wear depths penetrated the diffusion layer (Figure 9) an increase in friction is observed (Figure 7b). This is due to the different characteristics and non-ceramic properties of the now exposed diffusion zone. This trend gives a clear indication of the influence of the compound layer and diffusion zone on friction behaviour.

The compound layer mainly composed of ε –$Fe_{2\text{-}3}N$, detected using XRD (Figure 5b), is known for its high hardness and wear resistance which allows the application of large loads [19, 20]. The porosity present at the top of the compound layer is acknowledged for its ability to retain extra lubricant, combined with the presence of an oxide layer composed of magnetite (Fe_3O_4) acting as a running –in coating, would further enhance the samples friction abilities. The oxide layer is known for its low adhesion tendency due to its ceramic features which increases its wear resistance, contributing to further friction reduction [18, 19, 21].

With the MoS_2 coated samples the wear depths show that by the end of the 2 hour testing period the entire coating is almost removed, which is not entirely surprising as it is deemed to be a running-in coating as stated by the bonded coating manufacturer Klueber [9]. The durability of the coating is relatively short and once it has been worn through it cannot be replenished [17]. The substrate exposure is also a likely explanation why the friction results are comparable to that seen with the untreated samples and the slightly lower friction results seen may be due to the initial presence of a low friction coating and formation of low friction MoS_2 sheets. The substrate exposure could explain the significant higher volume loss when compared to the QPQ sample due to its lower hardness compared to the compound layer, Yue et al [1] proposed this also contributed to the low friction behaviour observed. Demydov *et al's* [22] study showed that MoS_2 nanoparticles delivered dialkyl dithiophosphate groups to wear points between interacting surfaces, causing these groups to decompose under high pressure and temperature, forming a protective polyphosphate tribofilm integrated with MoS_2.They believed that the synergistic interaction between the MoS_2 nanoparticles and polyphosphates accounted for the decrease in friction and wear observed. Due to an MoS_2 coating instead of MoS_2 nanoparticles being used in this study, the low friction results achieved in Demydov *et al's* [22] work were not achieved. Even though the MoS_2 coating was removed there were no particles remaining within the contact area to form low friction MoS_2 sheets as there would be with nanoparticles.

4.2 Surface Film Physical and Chemical Properties

The FIB-SEM investigation showed the formation of a glassy phosphate tribofilm on the MoS_2-coated and plain samples; whereas with the QPQ samples no clear phosphate layer was observed. Li *et al's* [23] research demonstrated that on softer substrates thicker and non-uniform films were formed, the irregularities of the film thickness were due to the deformation of the substrate, and this was common with softer surfaces. This deformation also resulted in rougher surface topographies. Within this study, plain samples had the lowest hardness (Figure 3), hence formed the thickest tribofilms (Figure 10c). Even though the MoS_2 coated samples had their coating removed the exposed substrate was of a higher hardness than the plain samples, which resulted in a thinner tribofilm being formed. Surface analysis of the plain samples showed them to have the highest post experimental roughness in comparison to the others. Yin et al [24] states that the interaction against a rougher counter face would provide greater opportunity for ZDDP to become trapped between the two surfaces, which would encourage the formation of thicker tribofilms. The presence of a hard and smooth layer due to the QPQ process can be deemed responsible for the development of a thin tribofilm on the samples surface. Spikes [6] research demonstrated that the thickness of the tribofilms formed were influenced by the elements present on the rubbing surfaces, with the absence of iron in the treated layers of the QPQ samples (Figure 5b – Fe profile) it is not surprising a thinner tribofilm is formed. XPS showed the presence of phosphorous and zinc elements (Figure 12) on the surface of QPQ samples indicating the presence of a thin anti-wear tribofilm.

The formation of a tribofilm when using ZDDP would be further hindered due to the presence of detergents and dispersants within the fully formulated oil used. Several researchers [25] have observed the deterioration of ZDDP's anti-wear properties in the presence of metallic detergents. This is due to the competition between the two additives for surface sites hence reducing the effective ZDDP surface concentration.

ZDDP Tribofilm Formation			
	Plain	**QPQ**	**Notes**
Mechanically Worked Film	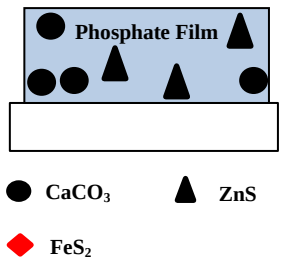	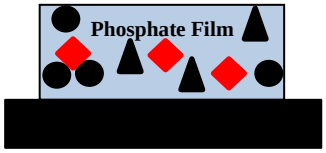	- ZnS indicates decomposition of ZDDP additive. - Free Fe^{2+} ions released due to mixing interact with sulphur to form FeS_2.

Figure 15. Schematic representation of tribofilms formed on plain and QPQ samples using fully formulated oil.

Literature [1] and experiments show that without the presence of anti-wear and extreme pressure additives in the hydraulic oil (base oil), QPQ samples demonstrated significantly higher wear. This is due to the absence of a glassy phosphate protective layer formed by the decomposition of the lubricant additives.

To investigate the role of the tribofilm and tribochemistry between the sample surfaces and lubricant in reducing friction during testing, XPS and Raman spectroscopy were used to characterize the formed protective layers. The initial presence of an organic species within the QPQ thermal film present was replaced with the formation of nitrides alongside organic species within the tribofilm after the surface was worn, possibly due to the removal of the oxide layer and the exposure of the

nitrided layer. With the QPQ samples the presence of hard nitrides within the tribofilm after the surface was worn may have further enhanced the wear resistance of the sample. FeS_2 was one of the key chemical species identified to be present in the QPQ tribofilms. Ito et al [26] proposed that with the presence of an iron oxide (Fe_3O_4) layer, above 60°C ZDDP molecules present in the lubricant would decompose creating free zinc ions. These free ions would adsorb on to the iron oxide surface, forming a zinc-rich, sulphur-free absorption layer ($ZnFe_2O_4$) that can grow without modifying the crystal structure of the surface. During testing, the sliding between two surfaces causes mechanical mixing to occur allowing Zn^{2+} and Fe^{2+} ions to exchange cations. Free iron ions are able to react with sulphur from the DDP^- forming iron sulphides and FeS_2. Figure 15 summarises schematically the chemical nature of fully formulated tribofilms formed on steel and QPQ samples.

Wada et al [27] concluded that the formation of large amounts of FeS_2, the greater the influence it would have on friction reduction, which is demonstrated in Figure 16. The presence of FeS_2 in the tribofilm combined with the QPQ compound layer could further enhance the samples friction reduction ability. FeS_2 had a greater presence in the QPQ sample tribofilms than plain and MoS_2-coated samples. However due to the relative thinness of the tribofilm the influence of FeS_2 on friction reduction could be negligible.

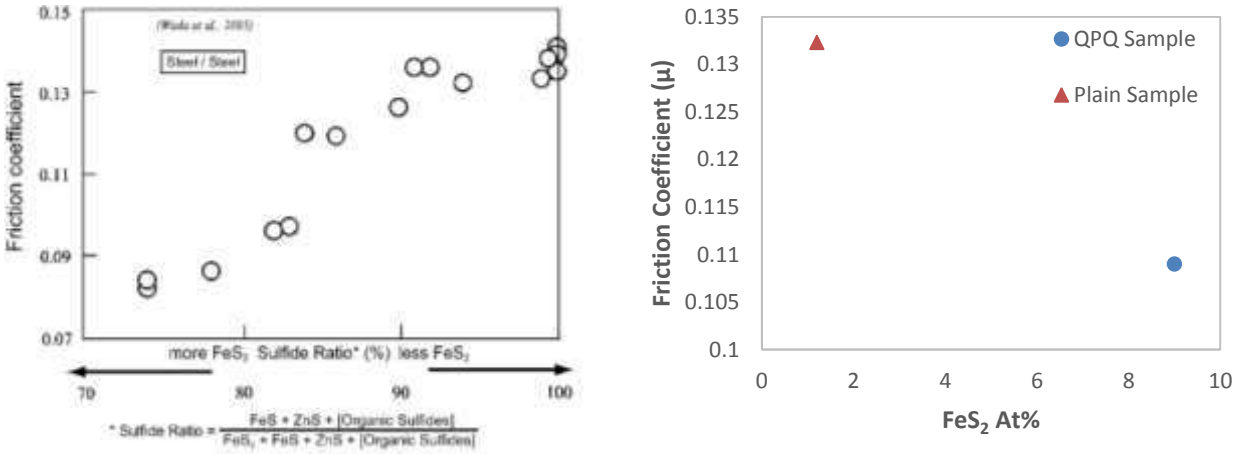

18

Figure 16. a) Effect of sulfides in tribofilm on friction coefficient [28]. **b)** At 1.19GPa contact pressure and 0.8min etching time.

This study's XPS analysis showed the formation of short chain length polyphosphates within the tribofilms of the QPQ samples. Shorter chained polyphosphates are regarded to enhance the mechanical and rheological properties of the surface giving it better tribological properties when compared to plain and MoS_2-coated samples which formed longer chained polyphosphates. Yue et al [1] suggested that the formation of a native iron oxide layer (Fe_2O_3) and nitrides on the nitrided surface would interact with the polyphosphates forming shorter chain lengths.

$$5\ Zn(PO_3)_2 + Fe_2O_3 \rightarrow Fe_2Zn_3P_{10}O_{31} + 2ZnO5\ (ZnO, P_2O_5)(Fe_2O_3, 3\ ZnO, 5\ P_2O_5) \quad (4)$$

The reaction highlighted in Equation 2 will result in de-polymerization, resulting in the formation of shorter poly-phosphate chain.

The presence of an iron oxide layer composed of Fe_3O_4 as in this study, would prevent de-polymerization occurring and the formation of longer chained poly-phosphates as seen with the formation of the QPQ samples thermal unworn film. This due to the cation exchange between the Fe^{2+}

and Zn^{2+} ions in the polyphosphate layer [24]. However the exposure of the nitrided layer may have led to the formation of shorter chained polyphosphates within the worn surface tribofilm. Similar behaviour was observed by Yue et al [1].

Heuberger et al [28] states that polyphosphates with two or three units of phosphates are possibly harder and tougher than longer chain lengths, and coupled with a hard nitride layer this would greatly reduce the wear rate, explaining the behaviour seen with the QPQ sample.

5. Conclusions

This study demonstrates the effectiveness of the oxy-nitriding heat process as a friction and wear control measure compared to other contemporary protective coating. The main conclusions that can be drawn from this study are as follows:

- The characteristics and mechanical properties of the layers formed by the oxy-nitrided treatment influenced the wear resistance and friction reduction behaviour observed. Through the removal of the compound layer, an increase in friction was observed, demonstrating the influence of the formed layers.
- The removal of the MoS_2 coating early on during testing, exposing the substrate of the sample greatly reduced the samples friction and wear reduction ability.
- The synergistic effects between the oxy-nitrided surface and the ZDDP additive showed to improve the wear characteristics of the samples through the formation of a protective anti-wear film.
- The formation of a Fe_3O_4 layer influences the formation of FeS_2 within the tribofilm.
- The presence of the nitrided layers with the QPQ sample influenced the formation of nitrides within the tribofilm after the surface was worn and the top oxide layer was removed.
- The presence of shorter phosphate chains and greater amounts of FeS_2 with the tribofilms formed on the QPQ samples could influence better mechanical and tribological properties. However due to the relative thinness of the tribofilms formed this effect could be negligible.

Acknowledgements

The authors would like to thank Komatsu Ltd and the University of Leeds for the funding of this project and the supplying of test samples and oils.

6. References

[1] Yue, W., et al., Synergistic Effects between Plasma-Nitrided AISI 52100 Steel and Zinc Dialkyldithiophosphate Additive under Boundary Lubrication. Tribology Transactions, 2012. **55**(3): p. 278-287.

[2] Manring, N.D., Friction Forces Within the Cylinder Bores of Swash-Plate Type Axial-Piston Pumps and Motors. Journal of Dynamic Systems, Measurement, and Control, 1999. **121**(3): p. 531-537.

[3] Nilsson, D. and B. Prakash, Investigation into the seizure of hydraulic motors. Tribology International, 2010. **43**(1–2): p. 92-99.

[4] Wang, Y. and S.C. Tung, Scuffing and wear behavior of aluminum piston skirt coatings against aluminum cylinder bore. Wear, 1999. **225–229, Part 2**(0): p. 1100-1108.

[5] Neville, A., et al., Compatibility between tribological surfaces and lubricant additives—How friction and wear reduction can be controlled by surface/lube synergies. Tribology International, 2007. **40**(10–12): p. 1680-1695.

[6] Spikes, H., The History and Mechanisms of ZDDP. Tribology Letters, 2004. **17**(3): p. 469-489.
[7] Crobu, M, et al, Effect of Chain-Length and Countersurface on the tribochemistry of Bulk Zinc Polyphosphate Glasses. Tribology Letters, 2012. **48**(3), p.393-406.
[8] Boβlet, J. Tufftride/ QPQ Process. [cited 2016 June]
[9] Klueber Lubrication Munchen, Bonded coatings for all metal surfaces. p.1-16.
[10] Perz Delgadi, Y., et al, Impact of wire-EDM on dry sliding friction and wear of WC-based and ZrO_2- based composites. Wear, 2011. **271**: p.1951-1961.
[11] Jacquet, P., J.B. Coudert, and P. Lourdin, How different steel grades react to a salt bath nitrocarburizing and post-oxidation process: Influence of alloying elements. Surface and Coatings Technology, 2011. **205**(16), p. 4064-4067.
[12] Yin, Z., et al, Application of soft X-ray absorption spectroscopy in chemical characterization of antiwear films generated by ZDDP Part I: the effects of physical parameters. Wear, 1997, **202**, p.172-191.
[13] Naumkin, A.V., et al., NIST X-ray Photoelectron Spectroscopy Database. [Online]. 2012. [Accessed 13 April 2015]. Available from: http://srdata.nist.gov/xps/Default.aspx
[14] Uy, D., et al., Soot-additive interactions in engine oils. Lubrication Science, 2010. **22**: p.19-36.
[15] El Mendili, E., et al., Phase transitions of iron sulphides formed by steel microbial corrosion. RSC Advances, 2013. **3** (48), p.26343-26351.
[16] Martin, J.M, et al., Superlubricity of molybdenum disulphide. The American Physical Society, 1993. **48**(14), p.583-587.
[17] Roberts, E.W., Thin solid lubricant films in space. Tribology International, 1990. **23**, p.95-104.
[18] Qiang, Y.H, et al, Microstructure and tribological properties of complex nitrocarburized steel. Journal of Materials Processing Technology, 2000. **101**, p.180-185.
[19] Holm, T and Sproge, L. Nitriding and Nitrocarburizing. Sweden . P.24.
[20] Karamboiki, C.M., et al., Influence of microstructure on the sliding wear behavior of nitrocarburized tool steels. Wear, 2013. **303**(1–2): p. 560-568.
[21] Lee, I., Post-oxidising treatments of the compound layer on the AISI 4135 steel produced by plasma nitrocarburizing. Surface & Coatings Technology, 2004. **188-189**, p.669-674.
[22] Demydov, D., et al, Advanced Lubricant Additives of Dialkyldithiophosphate (DDP)-Functionalized Molybdenum Sulfide Nanoparticles and Their Tribological Performance for Boundary Lubrication. Nanoscale Materials in Chemistry: Environmental Applications, 2010. **1045**, p.137-163.
[23] Li, Y-R., et al. The effect of Steel Hardness on the Performance of ZDDP Antiwear Films: A Multi-Technique Approach. Tribology Letters, 2008. **29**, p.201-211.
[24] Yin, Z., et al. Application of soft X-ray absorption spectroscopy in chemical characterization of antiwear films generated by ZDDP Part I: the effects of physical parameters. Wear. 1997, **202**, p.172-191.
[25] Wan, Y., Effects of detergent on the chemistry of tribofilms from ZDDP:studied by X-ray absorption spectroscopy and XPS. Tribology Series, 2002. **40**, p.155-166.
[26] Ito, K, et al. Formation mechanism of low friction ZDDP Tribofilm on Iron Oxide. Tribology Transactions, 2007. **50**(2), p.211-216.
[27] Ito, K, et al. Low-friction tribofilm formed by the reaction of ZDDP on iron oxide. Tribology International, 2006. **39** (12), p.1538-1544.

[28] Heuberger, R, et al. XPS study of the influence of temperature on ZnDTP tribofilm composition. Tribology Letters, 2007. **25** (3), p.185-196.